AIAA 2013-4250

Choosing Descent Flight-Path Angles for Small Jets: Case Study for the JFK Airport

Minghong G. Wu *
University of California, Santa Cruz, Moffett Field, California, 94035-1000
Steven M. Green†
NASA Ames Research Center, Moffett Field, California, 94035-1000

Descent planning for a small jet typically involves a fixed-flight path angle (FPA) descent. The selected FPA, however, is unknown to the air traffic controllers and can be far from optimal. Prior work identified three strategies for selecting/defining a fuel-efficient and flyable FPA for small jets. These three strategies vary in operational complexity and fuel-burn merits. The present work applies these strategies to small jets arriving at the JFK airport and compares the results to those from prior analysis of the DFW airport. Analysis of the fuel-burn merits of the three strategies was performed using a full year of track data as well as the forecast winds in 2011. Parameters of the strategies were adapted to directions of arrival and timespans of a year. Results showed that the Airport-Static adaptation of the Universal FPA strategy burns on average 21.5 lbs more fuel per flight than the Min-Fuel FPA solution. Up to 74% of this extra fuel burn can be recovered by adapting the FPA selection to the arrival gate, day, and descent speed. Compared to results for the DFW airport, the high-altitude restrictions for JFK, directions of arrival, and winds were found to be among the leading factors that influenced the relative fuel-burn merits of the three strategies.

Nomenclature

ΔP	Percentage difference in extra fuel burn
γ	Inertial flight-path angle
γ_0	Descent-Speed FPA's baseline descent flight-path angle
γ_{univ}	Universal FPA's descent flight-path angle
CAS	Calibrated airspeed
CDA	Continuous Descent Arrival
CTAS	The Center-TRACON Automation System
DCAS	Descent calibrated airspeed
DFW	Dallas/Fort Worth International Airport
EDA	Efficient Descent Advisor
FMS	Flight Management Systems
FAA	Federal Aviation Administration
FPA	(Inertial) flight-path angle
f_i	Scaled fuel burn
f_0	Raw fuel burn
JFK	John F. Kennedy International Airport
LAX	Los Angeles International Airport
N_{r}	Number of RUC weather forecasts
NAS	National Airspace System
N_i	Number of passenger seats

*Research Engineer, AIAA Member
†Aerospace Engineer, AIAA Associate Fellow

RUC	Rapid Update Cycle
STA	Scheduled time of arrival
TMA	Traffic Management Advisor
TOD	Top of descent
TS	Trajectory Synthesizer

I. Introduction

While much research over the past two decades has been directed at efficient arrival operations into the constrained terminal airspace, particular case studies and field trials have focused on large commercial transport jets.[1–3] Small jet types (regional, business, and light) present additional challenges, and are a large and potentially high-growth portion of NextGen traffic operations in the United States.[4] Unlike large commercial transport jets, which are equipped with performance-based Flight Management Systems (FMS) that attempt to optimize the vertical profile with near-idle descents, small jets are equipped with kinematic FMS that have simpler vertical navigation capabilities. Descent planning for these jets typically involves an inertial fixed-flight path angle (FPA) descent that is either based on a company-programmed default or a pilot-selected value. The selected FPA is minimally adapted to wind and can be fuel-inefficient and/or difficult to fly. Moreover, the FPA is not known to the air traffic control and therefore cannot be incorporated as intent information by the ground decision support tools in trajectory prediction. Since the selection of an FPA essentially defines the top-of-descent (TOD) location, a key event for evaluating trajectory prediction accuracies, such intent information can be crucial to ground-based separation assurance algorithms[5] and to achieving fuel-efficient descents in congested airspace.[6]

It is desirable to develop a standard procedure for establishing efficient descent FPAs for small jets in transition airspace, especially in a high-density air-traffic environment. Such selections of FPA, when simultaneously known between the flights and the ground control facilities, are expected to realize better trajectory predictability, which in turn would support the Trajectory Based Operations and increase airspace throughput. Specifically, a procedure for defining an FPA was required to enable the Efficient Descent Advisor (EDA), which was developed to assist en-route controllers achieve fuel-efficient continuous descent arrivals (CDA)[7] that both meet the Traffic Management Advisor's[8] scheduled times of arrival (STAs) and maintain separation during congested operations.

Previous work by the authors proposed and analyzed three FPA selection strategies:[9] Universal FPA, Descent-Speed FPA, and Min-Fuel FPA. While all three are expected to achieve the same level of trajectory predictability, they vary in operational complexity and fuel efficiency. To compare their relative fuel-burn merits, methodologies were developed and applied to the Dallas/Fort Worth International Airport (DFW). Results showed that a carefully selected universal FPA for all flights lead to descents that consume 26 lbs of extra fuel burn per flight compared to the Min-Fuel FPA strategy that selects an FPA for each flight dynamically. To avoid planned speed-brake usage, the Universal FPA selects a shallow FPA to ensure speed-brake-free descents for the majority of flights at the cost of fuel-efficiency. These fuel effects were reduced by adapting the selection of FPA to season, month, day, and/or the four arrival gates of DFW, and the resulting fuel burn approached that of the minimum fuel FPA, getting within 9 lbs when the descent speed was also taken into account. Since the results are specific to DFW, analysis of another airport in the US would shed light on the sensitivity of the relative fuel-burn merits of the three strategies to various environmental and airport-configuration factors.

The purpose of this paper is to apply the methodologies for selecting the descent FPA to the John F. Kennedy International Airport (JFK) and to compare the results with those for DFW. The results and comparison will help generalize the FPA selection process to major airports in the United States. JFK is different than DFW in terms of its wind magnitude, altitude restrictions, and arrival flight directions. All these characteristics were expected to affect the relative fuel-burn merits of the three strategies. The similarities and differences between these two airports will be further discussed in subsequent sections.

The rest of this paper is organized as follows: Section II reviews the three proposed FPA strategies, the methodology for parameter selection, and the adaptation of the first two strategies to direction (arrival gate) and timespans; Section III presents the wind analysis that identifies JFK as the airport with strongest wind variation and discusses specifics about JFK arrival traffic; Section IV describes the modeling schemes for the metered arrival trajectories in the transition airspace; Section V presents results of the selected FPAs in various adaptations and compares fuel burn between the three strategies; Section VI compares the results

for JFK to those for DFW and investigates major factors that contributed to their differences; and, finally, Section VII summarizes the findings in this work.

II. Three FPA Selection Strategies

In previous work, three strategies were proposed to define the fixed FPA for small jet arrivals under metering conditions.[9,10] The three strategies were as follows:

1. Universal FPA - defines an FPA for all flights
2. Descent-Speed FPA - defines the FPA as a function of the descent speed
3. Min-Fuel FPA - computes a custom FPA for each flight

Universal FPA defines a universal FPA for all small jets arriving to an airport, gate, or route. This is akin to a glide slope extending from the first altitude constraint on the Standard Terminal Arrival Route (STAR) back up to the top of descent (TOD) in the en-route airspace. The advantage of Universal FPA is its simple form, which allows it potentially to be published as part of the arrival procedure. The disadvantage is that it does not account for the effects of descent speed and winds on the fuel efficiency or the range of flyable FPAs.

Descent-Speed FPA takes into account the effects of the descent speed on the range of fuel-efficient and flyable FPAs. During periods of high density traffic, controllers would issue speed clearances for each arrival flight, and EDA supports clearances that give both cruise and descent speeds. One the descent speed is relevant to the selection of FPA. This FPA function reduces the FPA by 0.1° for every 10 knot increase of descent calibrated airspeed (CAS). Note the FPA is negative for descents, and reducing the FPA makes it steeper. It was observed that this rate of change of FPA with respect to the descent CAS captures the variation of fuel-efficient FPAs with speed.[10] The change of 0.1° matches the precision of FPA-selection increments typical of small jet avionics.[11] The FPA function is defined by Equation 1:

$$\gamma = \begin{cases} \gamma_0 & \text{, if DCAS} < 255 \\ \gamma_0 - 0.1 & \text{, if } 255 \leq \text{DCAS} < 265 \\ \gamma_0 - 0.2 & \text{, if } 265 \leq \text{DCAS} < 275 \\ \ldots, & \end{cases} \tag{1}$$

where γ is the FPA in degrees, DCAS is the descent CAS in knots, and the adaptive parameter γ_0 stands for the value of γ at 250 knots descent CAS, a typical speed expected at the metering fix. Note the selection of the parameter γ_0 defines the entire FPA function. Descent-Speed FPA is expected to be more fuel-efficient than Universal FPA by accounting for the descent speed. Both Universal FPA and Descent-Speed FPA have the disadvantage that they do not account for the effects of the direction of the winds aloft on the range of fuel-efficient and flyable FPAs.

While Universal FPA and Descent-Speed FPA define the FPA and the FPA function ahead of time, Min-Fuel FPA computes the minimum-fuel FPA to be communicated explicitly to the pilot of each flight just prior to the TOD. The computation is based on the route, winds and temperature aloft, and the speed profile necessary to meet the STA. Figure 1 sketches the fuel burn as a function of the descent FPA for a typical flight. While the requirement of communicating the FPA to the pilot in real time may make Min-Fuel FPA infeasible to implement without controller/pilot data-link, it serves as a reference point for fuel burn comparison with the first two strategies.

II.A. Planned Speed-Brake Usage

In addition to predicted fuel burn, the selection of FPA also takes into account uncertainties in vertical profile planning. To keep the aircraft on the planned vertical path, power adjustment is preferred to speed-brake deployment for reasons of passenger comfort and the desire of pilots to reserve the use of a speed brake for rare occasions. Therefore, the analysis of trajectories was limited to those FPAs that do not require planned speed-brake usage.

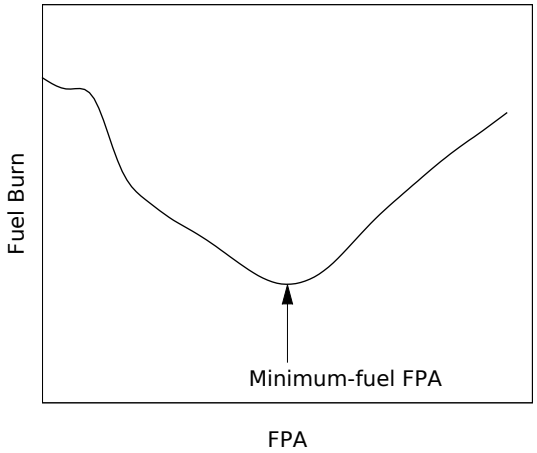

Figure 1. The Min-Fuel FPA strategy selects the minimum-fuel FPA.

II.B. Parameters in Universal FPA and Descent-Speed FPA

The universally fixed FPA in Universal FPA, denoted as γ_{univ}, and the γ_0 in Descent-Speed FPA are parameters that must be selected carefully, with consideration for the prevailing winds aloft and, to a lesser extent, the anticipated traffic demand. The following selection criteria are applied:[9,10]

1. For the parameter considered, at least 99% of the flights have feasible trajectories, meaning trajectories that have speeds within the performance envelope and do not require speed brake usage.

2. The parameter should result in the least average fuel burn per flight.

The first criterion defines the steepest parameter that can be selected, and the second criterion selects a minimum-fuel FPA from those parameters no steeper than the steepest parameter allowed by the first criterion.

II.C. Adaptation of Universal FPA and Descent-Speed FPA

While steeper FPAs are typically more fuel-efficient for arrival flights in a headwind, they can be unflyable for flights in the opposite direction. A shallow FPA would guarantee flyability for both directions, but will be fuel-inefficient for flights in a headwind. These observations motivated the adaptation of γ_{univ} and γ_0 to the direction of arrival. Compared to a static implementation, adaptation to the direction of arrival achieves a greater degree of "customization" and can improve fuel efficiency. While adaptation to the direction of arrival reduces the variation of along-track winds due to directions, it does not mitigate the variation of winds over time. The fuel efficiency of the Universal FPA and Descent-Speed FPA strategies can be further improved by adapting γ_{univ} and γ_0 to seasonal norms, monthly norms, or even daily predictions.

A set of systematic, temporal and location/directional adaptations was proposed in previous work[9] and reviewed here in Table 1. The columns represent different levels of adaptation for different airspaces, starting with a basic "one size fits all" adaptation for all airports across the National Airspace System (NAS). Moving to the right, each column represents a progressively finer adaptation of the FPA strategy to a specific airport, individual arrival gates (corner posts) feeding an airport, all the way down to specific arrival routes feeding each arrival gate. The rows represent a temporal scale starting at the top with the simplest option of a static adaptation. Moving down, each row represents a progressively finer adaptation to account for changes in the prevailing winds as a function of season, month, day or even hour. The table illustrates the overall approach and potential scope. For the purposes of this paper, the analysis will assess the eight types highlighted and numbered in the table. The analysis of adaptations at the NAS-wide level, or at the level of specific arrival routes and/or hours of the day, are left for future work. Table 2 lists the names given to these eight adaptation types analyzed in this work:

Table 1. The types of adaptations categorized by their granularity in location/direction and time

	Airspace/Direction			
Time	NAS	Airport	Arrival Gate	Arrival Route
Static		1	5	
Season		2	6	
Month		3	7	
Day		4	8	
Hour				

Table 2. The eight adaptation types analyzed for the JFK traffic

#	Name	FPA/FPA Function Defined for
1	Airport-Static	the airport
2	Airport-Season	the airport by season
3	Airport-Month	the airport by month
4	Airport-Day	the airport for each day
5	Gate-Static	each arrival gate
6	Gate-Season	each arrival gate by season
7	Gate-Month	each arrival gate by month
8	Gate-Day	each arrival gate for each day

III. Selection of Case Study: JFK

The selection of John F. Kennedy Airport (JFK) was motivated by multiple factors. The major factor was the search for an airport that has strong wind variations. Wind along the route acts as a major discriminator in selecting the descent FPA for an arrival flight. Stronger variation of winds among directions of arrival increase the benefits of adapting to the directions of arrival. Stronger variation of winds across timespans increases the fuel-burn merit of adapting the FPA selection to season, month, and day. Previous analysis of the DFW airport showed fairly strong seasonal variation of winds. However, other major airports in the United States may have even stronger directional and temporal variation of winds, and JFK was expected to be an example of such.

To compare the variation of winds along the route among some major airports in the United States, winds along the route were estimated for four hypothetical arrival routes constructed for each airport. Four hypothetical points in space at four corners around an airport, NE, NW, SE, and SW, were selected at 150 nmi each from the airport and at 35,000 ft in altitude. The vectors connecting each point to the airport defines the four hypothetical directions of arrival. Wind components along the vectors were estimated using the two-hour, 40 km Rapid Update Cycle (RUC) weather forecast[12] for year 2011. The wind forecast was generated on an hourly basis, amounting to more than 8660 forecast winds (a few days of RUC were not available). Two quantities were calculated from the wind components to represent the wind variations across directions and timespans. Let N_r denote the number of available RUC wind estimates. The standard deviation of the average wind along each of the four directions is defined by Equation 2:

$$\sigma_{\mathrm{dir}}{}^2 = \frac{1}{4}\sum_{i=1}^{4}(\overline{W_i} - \mu)^2, \text{ where } \mu = \frac{1}{4}\sum_{i=1}^{4}\overline{W_i}. \tag{2}$$

Here $\overline{W_i}$ is the average of the N_r wind components along a direction i, defined by Equation 3:

$$\overline{W_i} = \frac{1}{N_\mathrm{r}}\sum_{j=1}^{N_\mathrm{r}} W_{i,j}, \tag{3}$$

and $W_{i,j}$ denotes the wind component estimated using RUC wind file j along direction i. The average of

the standard deviation of wind for each direction is defined by Equation 4:

$$\sigma_{\text{time}}{}^2 = \frac{1}{4}\sum_{i=1}^{4}\sigma_i{}^2, \text{ where } \sigma_i{}^2 = \frac{1}{N_{\text{r}}}\sum_{j=1}^{N_{\text{r}}}(W_{i,j} - \overline{W_i})^2. \tag{4}$$

Note that, although only standard deviations were calculated, the wind distribution may not be exactly Gaussian and outliers may have effects on the fuel merits of the FPA selection strategies. Further investigation of the wind distribution is left for future work.

While σ_{dir} is indicative of the benefits of adapting the descent FPA to flight directions, σ_{time} is indicative of the benefits of adapting the descent FPA to timespans. Figure 2 shows the estimated wind variations, σ_{dir} and σ_{time}, around twelve major airports in the United States. The airports in this figure are ordered

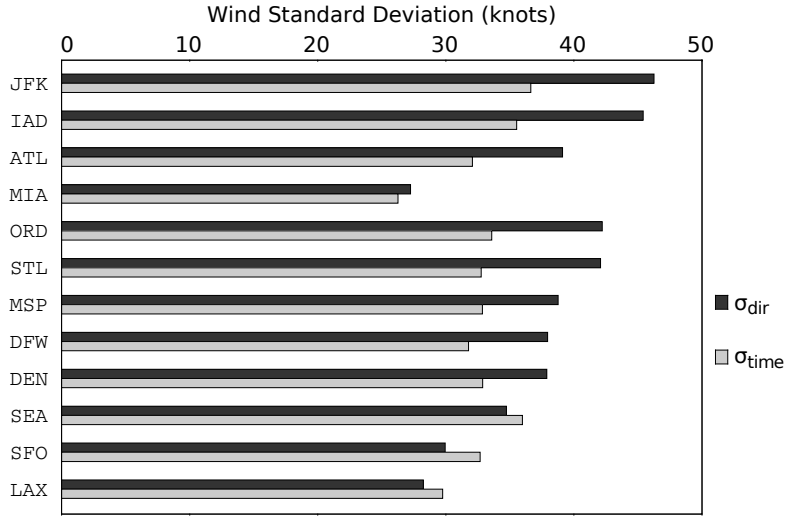

Figure 2. Variation of winds aloft at twelves major airports in the United States for 2011.

from east to west and from north to south. JFK has the highest variation of both types and hence was chosen as the subject of this analysis. LAX and MIA experience significantly weaker winds and can be the subject of another study. The airport analyzed in previous work, DFW, ranked 8th in σ_{dir} and 11th in σ_{time} among the twelve airports. The rank for σ_{time} was a bit surprising since the jet stream passed through DFW in winter and resulted in clear seasonal variations. Nonetheless, the definition of σ_{time} accounts for wind variation on a per-hour basis and the seasonal variation was not directly captured by this definition.

Figure 3 shows the wind components along the four hypothetical directions of arrival leading to JFK as a function of time of year, 2011. While flights from the NW and SW clearly would experience tailwind most of the time, flights from the NE and SE would experience mostly headwinds. Extremely strong winds were observed for SW and NE during some early hours of February 7, when the SW direction had up to 166 knots of tailwind and the NE had up to 172 knots of headwind. It will be shown later that these strong winds on this day had interesting effects on the selected FPA and FPA function.

Two of the four STARs leading to JFK have restrictions at high altitudes due to the congested airspace in the New York metroplex area. Figure 4 shows arrival tracks of small jets on January 7th, 2011. Each arrival jet aircraft enters the Terminal Radar Approach Control Facilities (TRACON) through one of the four arrival STARs, characterized by the waypoints CCC, CAMRN, HARTY, and LOLLY, respectively. These four points are the most upstream points in the STARs that have altitude restrictions, which are summarized in Table 3. Note that the speed restrictions are defined in terms of calibrated airspeed (CAS). Flights from the N and NW must capture the high-altitude restrictions of 20,000 and 21,000 ft, respectively, when they cross LOLLY and HARTY. Additional downstream altitude and speed restrictions apply, making the vertical profile beyond LOLLY and HARTY very constrained. For this work, only the portion of the flight trajectory from cruise to one of these four points is considered for varying the FPA. This reduction in descent altitude change is expected to diminish the fuel burn differences observed among different values

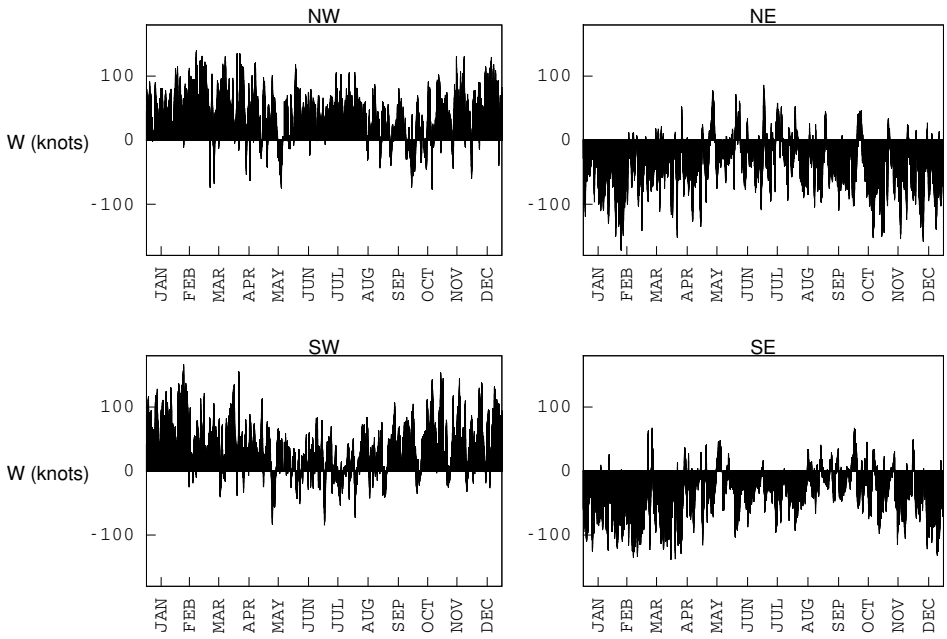

Figure 3. Wind along the hypothetical routes for the JFK airport. A positive wind is a tailwind.

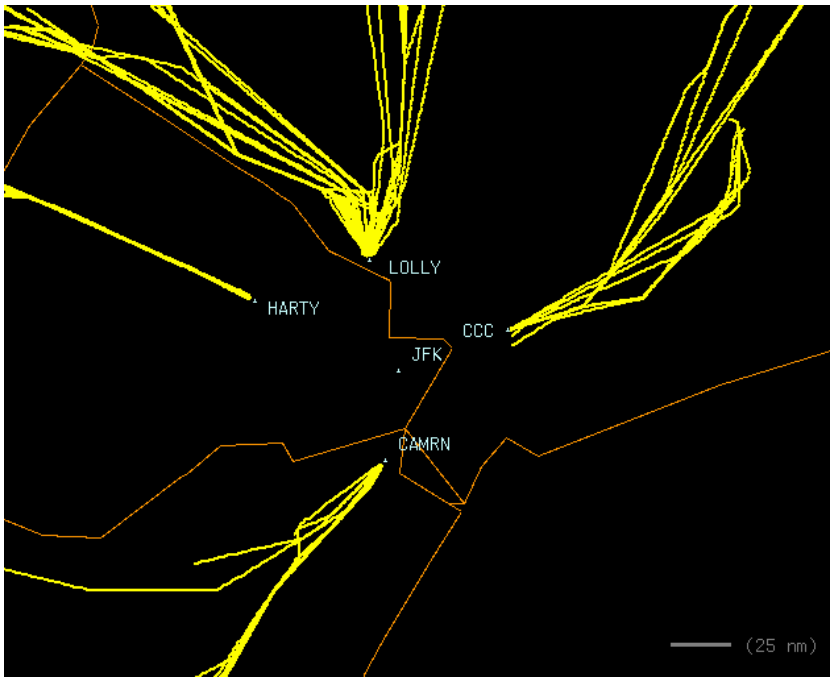

Figure 4. Tracks of arrival small jets to JFK on January 7, 2011.

of the descent FPA, and hence diminish the difference in the relative fuel-burn merits of the three selection strategies.

Unlike DFW studied in prior work, which has two-thirds of its small jet arrivals from the east, 70% to 80% of JFK's small jet arrivals are from the west, in directions of NW, W, or SW. Although JFK has a small number of arrival flights from NE, very few small jet flights approach from SE, which is over the Atlantic Ocean. Since the fuel burn of the trajectory is less sensitive to the selected FPA in the headwind than in the tailwind,[10] the difference in the distribution of directions of arrival between JFK and DFW will change the

Table 3. The first altitude and/or speed restrictions along the STARs for JFK

Waypoint	Altitude (ft)	Speed (CAS in knots)
CCC	12,000	250
CAMRN	12,000	250
LOLLY	20,000	-
HARTY	21,000	-

relative fuel-burn merits of the three strategies. Besides, the uneven distribution of the directions of arrival for JFK may diminish the benefits of adapting the selection of descent FPAs to the flight directions when compared to DFW.

IV. Analysis Approach

The methodologies for selecting the FPAs and the modeling schemes have been described in detail previously.[9] The following sections briefly review them for completeness of this paper.

IV.A. Calibrating and Comparing the Three Strategies

The methodology that compares the benefits of the three strategies consists of two conceptual parts: first select the parameters for the Universal FPA and Descent-Speed FPA strategies, and then compare the fuel burn between the three strategies for a set of traffic and wind conditions.

The first part of the methodology determines the parameters of Universal FPA and Descent-Speed FPA using estimates of winds and temperatures aloft, traffic demand, and modeled metering delays. The second part of the methodology estimates and compares the fuel burn of the strategies, using the estimates of winds and temperatures aloft, actual traffic data, and modeled or actual metering delays. While the estimates of winds, temperatures aloft, and traffic demand for the second part need not be the same as that used for the first step, they are the same in this analysis, being the RUC data and the track data of JFK recorded in 2011. Since the same estimates of winds and temperatures aloft and traffic demand were used in both parts of the methodology, the fuel burn and planned speed-brake usage recorded in the first part for selecting the parameters of γ_{univ} and γ_0 can be directly used in the second part without having to recalculate them.

The implementation of the methodology combines the two conceptual parts into one run of a fast-time simulation as described in detail in the following sections. For each arrival flight and a modeled metering delay, the analysis computes a set of meet-time trajectories with varying FPA and descent CAS profile. Because the FPA selected by each strategy must be from these trajectories, the analysis of these trajectories was sufficient for the fuel burn comparison between the three strategies.

For adaptations to longer timespans, the relative fuel-burn merits of the Universal FPA and Descent-Speed FPA strategies would be optimistic compared to those attainable in actual implementation. This is because the high-fidelity weather, and flight plan information accessible in real time to Min-Fuel FPA were used for selecting their parameters, while in actual implementation only crude forecasts are available for longer timespans.

IV.B. Route and Vertical Profile

Trajectories are constructed for arrival flights to JFK that enter the terminal airspace through one of the four points, CCC, LOLLY, HARTY, and CAMRN, shown in Figure 4, that were treated as "pseudo" metering fixes. While JFK currently does not meter the arrival flights, controllers issue speed clearances to sequence the arrival flights while maintaining their spacings during periods of high traffic density. Therefore, arrival flights into JFK can effectively be modeled as if they were in an metered environment. In this analysis, the terms "metering fix" and "gate" have a one-to-one mapping and are used interchangeably. A distance-based freeze horizon of 160 nmi was assumed, inside of which TMA would fix the STA for the aircraft.[13] The selection of 160 nmi guaranteed that the TOD is inside the freeze horizon and each trajectory has cruise and descent phases. The initial condition was selected at a corresponding track point nearest the

freeze horizon. For simplification, direct trajectories from the initial point to the metering fix were assumed without actually parsing the flight plans for the waypoints. The crossing restrictions shown in Table 3 for the four pseudo metering fixes were modeled at the end of the trajectories.

Figure 5 illustrates a typical vertical profile that has five segment types distinguished by altitude changes and pilot procedures. Individual trajectories will contain all or a subset of these segments depending on the speed profile needed to meet the STA. Each segment is modeled kinetically by fixing two control parameters.

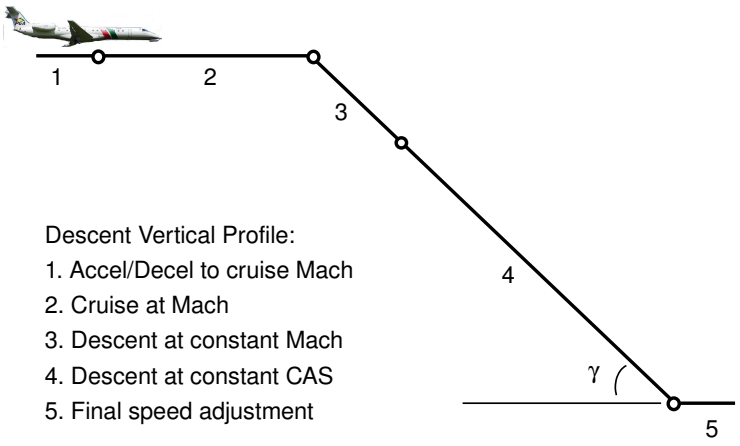

Figure 5. A general vertical profile that contains five segment types.

One of the parameters is the FPA; the second depends on the segment. For a cruise segment the model fixes the airspeed or the engine control for acceleration or deceleration. For the constant-speed descent segments, the model fixes an airspeed in Mach or CAS.

IV.C. Aircraft and Fuel Burn Modeling

The Trajectory Synthesizer (TS) component[14,15] of the Center-TRACON Automation System (CTAS)[16] was used to compute trajectories, their associated fuel burn, and the planned speed-brake usage. While a detailed performance model of small jet types would have been desirable, one was not available. Instead, a high-fidelity, CTAS model for a mid-size, narrow-body, twin-jet airliner with a typical descent weight of 170,000 lbs was used. The speed envelopes were selected within the ranges of small jets. To capture variation of descent performances due to weight differences, the weight for each flight was selected randomly from a normal distribution with a standard deviation of 8,400 lbs.

To account for the variation of the fuel-burn rate among aircraft types, the fuel burn was scaled by the empirical formula

$$f_i = f_0 * \frac{N_i + 30}{230}, \tag{5}$$

where f_i is the scaled fuel burn; f_0 is the raw fuel-burn rate calculated by CTAS for the mid-size, narrow-body, twin-engine jet; and N_i is the number of passenger seats typical of the aircraft type i. This empirical formula was derived by taking the linear regression of the nominal cruise fuel-burn rate of eight small jets plus the mid-sized twin engine jet, using the Base of Aircraft Database (BADA) 3.8 performance model.[17] Although BADA provides modeling parameters for small jets, the calibration of these parameters focused on nominal flight conditions only. Since the analysis in this work explored a wide range of the speeds, containing both nominal and off-nominal ones, it was decided that the high-fidelity CTAS model with scaled fuel burn was more appropriate for the fuel-burn analysis.

IV.D. Metering Delay

The delay at the metering fix for each flight was selected randomly from a uniform distribution between zero and the maximum delay that can be absorbed by speed reductions. The delay time was added to the nominal time in order to specify the STA at the metering fix for a flight. By definition, a flight with nominal cruise and descent speeds would arrive at the metering fix with zero delay. A flight with minimum cruise

and descent speeds would arrive at the metering fix with maximum delay. Idle thrust descent was assumed for these two trajectories.

IV.E. Fixed-FPA Meet-Time Trajectories

A set of meet-time trajectories with varying FPA and descent CAS profile was computed for each flight using a modeled metering delay. Only the meet-time trajectories that do not have planned usage of speed brakes are included for the analysis. Fuel burn was calculated for each meet-time trajectory. These meet-time trajectories provided all the fuel-burn data needed for comparison of the three strategies, because each of the three strategies must select an FPA from these meet time trajectories.

For descent FPAs ranging from -1.8° to -5.5°, with an increment of 0.1°, a meet-time algorithm attempted to compute a fixed-FPA trajectory for each value of the FPA. The meet-time algorithm iterated cruise and descent speeds until the trajectory met the desired time-to-fly within a tolerance of 2 seconds. Cruise and descent speeds were related by the Cruise-Equals-Descent speed mode developed for EDA.[18] The resulting meet-time trajectories have different combinations of FPA-descent-CAS pairs. All three strategies were applied to select FPAs. If no meet-time trajectories had the FPA defined by Universal FPAor satisfy the FPA-descent-CAS relationship defined by Descent-Speed FPA, a failure was recorded for this parameter of the strategy. The number of failures, usually resulting from speed brake usage or speeds going out of bounds, was used to determine whether the candidate parameters γ_{univ} and γ_0 should be rejected (See Section II.B).

IV.F. Simulation and Data Analysis

A fast-time Monte Carlo simulation was performed to generate the meet-time trajectories for small jet arrivals to JFK. For each arrival flight, a descent weight and a delay time were sampled from the distributions described in Sections IV.C and IV.D. The meet-time algorithm computed a set of fixed-FPA meet-time trajectories for the specified test condition, using the RUC data in the TS calculation of the trajectories. The fuel burn and speed-brake usage were recorded for further analysis to be described below. All data were categorized by gates and days.

The selection criteria described in Section II.B were used to select γ_{univ} and γ_0 for each of the eight adaptation types listed in Section II.C. The analysis selected γ_{univ} for Universal FPA from values between -1.8° and -5.5° with increments of 0.1°. The analysis selected γ_0 for Descent-Speed FPA from values between -1.8° and -3.7° with increments of 0.1°. The steepest parameters were selected such that all speed-brake-free trajectories in any wind condition were analyzed. The shallowest parameters were selected such that the route has enough path distances for the cruise phase. For each γ_{univ} and each γ_0, the average fuel burn per flight and feasibility rate were computed from results of all flights. The feasibility rate was defined as the ratio of the flights with flyable FPAs (total number of "success") to the total flights analyzed. It must be 99% or better for γ_{univ} or γ_0 to be selected. For the Airport-Static adaptation, all flights were analyzed for the selection. For other adaptations, a subset of the flights was analyzed to select γ_{univ} or γ_0 for a gate and/or a timespan. For example, a total of sixteen pairs of γ_{univ} and γ_0 were selected for the Gate-Season adaptation (four gates times four seasons), each using the flights into a specific gate during a specific season.

Selection of the parameters based on the feasibility rate ensures that the vast majority of flights will have flyable FPAs, but it does not consider the variation of winds that can make the flights through some gates on some days particularly difficult to fly. To ensure the feasibility rate for any given day and gate was "tolerable" for adaptations that have longer timespans or are airport specific, another feasibility rate of 80% or better for any pair of gate and day was required.

Once the parameters were selected, each strategy would select an FPA for each flight. The extra fuel burn for the FPAs selected by Universal FPA and Descent-Speed FPA were computed for all flights as a metric for the relative fuel-burn merits between the three strategies.

V. Results

Results of the fast-time simulation are presented as follows: Section V.A summarizes the statistics of the number and aircraft types of the arrival flights used in the simulation. The following sections discuss results for each strategy, starting from Min-Fuel FPA because it revealed distributions of the individually selected FPAs among flights. Section V.B shows the selected FPAs for flights using Min-Fuel FPA, the minimum-fuel strategy, and discusses their correlation with winds. Sections V.C and V.D show the selected FPA and

FPA function for Universal FPA and Descent-Speed FPA, respectively, in the gate-specific adaptation types. Section V.E compares the fuel-burn merits of the three strategies.

V.A. Arrival Flights

Table 4 shows the total number of arrival flights of small jets identified and used in this analysis. Due to occasional periods when the data feed was unavailable, the track data was missing for 13 of the 365 days. Among the days where the track data was available, some data were not recorded due to short interruptions

Table 4. Total number of arrival flights of small jets

Month	Days	CCC	LOLLY	HARTY	CAMRN	Missing Days
Jan	31	541	1133	906	1464	
Feb	20	290	658	536	847	1, 21-25, 27-28
Mar	31	598	1196	1010	1675	
Apr	30	555	1147	1109	1626	
May	29	491	1207	1110	1481	21-22
Jun	30	635	1285	1192	1496	
Jul	30	824	1258	1229	1581	16
Aug	28	743	1149	1132	1415	21, 27-28
Sep	30	681	1371	1234	1669	
Oct	31	603	1284	1206	1747	
Nov	30	469	1039	1124	1719	
Dec	31	405	940	971	1610	
Total	351	6835	13667	12759	18330	

of the data feed. The CAMRN gate was the busiest, accounting for 36% of the small jet arrival flights.

Figure 6 shows the most frequent small jet aircraft types observed among the 51,591 arrival flights. The Embraer ERJ 190 and Bombardier CRJ 200 accounted for more than 48% of the fleet, with the other 58 aircraft types making up the rest.

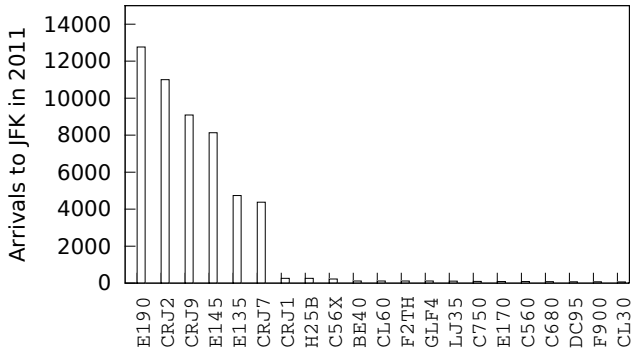

Figure 6. Most frequent arrival small jet types observed arriving at the JFK in 2011.

V.B. Min-Fuel FPA

Min-Fuel FPA selects a minimum-fuel FPA for each flight. Figure 7 presents distributions of the FPAs selected for flights using Min-Fuel FPA on a per-day basis. Among the four gates, the steepest FPAs were selected for CCC, ranging from -2.9° to -3.6° in winter time and from -2.7° to -3.2° in summer time. The other three gates have shallower FPAs selected, with the fluctuations stronger for flights to LOLLY. This is most likely due to a wider variation of the headings of the arrival flights to LOLLY (See Figure 4). Since steeper FPAs are typically selected in the presence of strong headwinds,[9] the results suggest that flights into CCC experience mostly strong headwinds throughout the year. This is in strong correlation to the wind along the route for the NE direction of JFK shown in Figure 3. In addition, seasonal variation of the selected FPAs was clear for CCC in Figure 7. The same variation is also visible in the other three plots, although subject to more fluctuation.

It is interesting to see that the very shallow -1.8° was the minimum-fuel FPA for some flights, even in the presence of headwinds as for CCC and LOLLY on Feb. 7, 2011 (shown in the dip of the first quartile

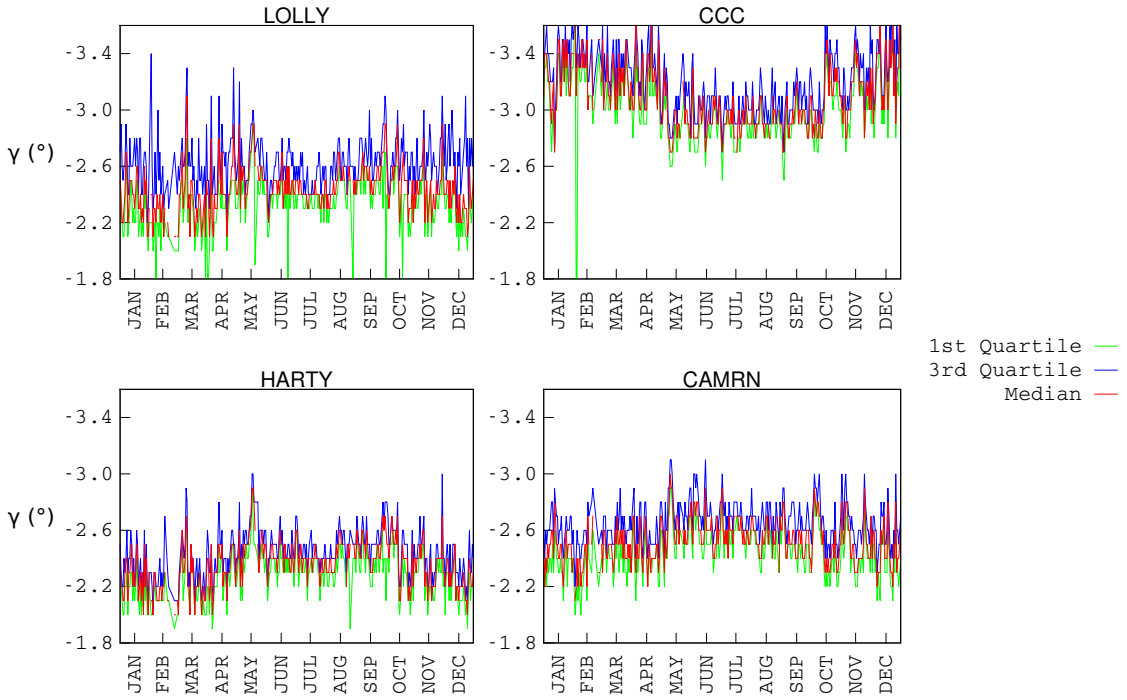

Figure 7. The first quartile, third quartile, and median FPAs selected using Min-Fuel FPA.

curve). This inversion of minimum-fuel FPA towards a shallow value can happen for certain combinations of headwinds along with favorable wind gradients with respect to altitude and has been discussed previously.[9]

V.C. Universal FPA

Universal FPA selects the FPA based on the average fuel burn per flight and the feasibility rate. Figure 8 shows values of γ_{univ} selected for the gate-specific adaptations of Universal FPA. The airport-specific FPAs are not shown but their fuel burn will be analyzed in Section V.E. Compared to Min-Fuel FPA, similar trends were observed in the selected FPA using Universal FPA as the steepest FPAs were selected for CCC. The FPAs selected for HARTY are the shallowest of all gates. Regarding the Gate-Day adaptation on February 7, -1.9° was selected for CAMRN while -1.8° was selected for CCC. The former FPA was selected because any steeper FPA would result in too many speed-brake demanding trajectories while the latter was selected because it results in better fuel burn than any steeper FPAs. The same shallow angle of -1.8° was also selected for CCC on January 12, February 3, February 4, and March 30. For CCC on February 7, the nineteen flights analyzed all have flyable trajectories for all the values of FPA from -1.8° to -3.4°. The extra fuel burn computed for each FPA ranged from 2.5 lbs to 6.9 lbs, with the lowest extra fuel burn of 2.5 lbs yielded by the FPA of -1.8°. The FPA that yielded the second lowest extra fuel burn was -3.3° with an extra fuel burn of 3.0 lbs, and can be a reasonable choice of FPA as well.

V.D. Descent-Speed FPA

Figure 9 shows values of γ_0 selected for the gate-specific adaptations of Descent-Speed FPA. The airport-specific FPA functions are not shown here, but their fuel burn will be analyzed in Section V.E. The selected values of γ_0 are very similar to γ_{univ} selected for Universal FPA. The steepest values of γ_0 were selected for CCC. Similar to Universal FPA, a shallow value of -1.8° was selected for γ_0 for both CCC and CAMRN for the Gate-Day adaptation on February 7 for reasons described in previous sections.

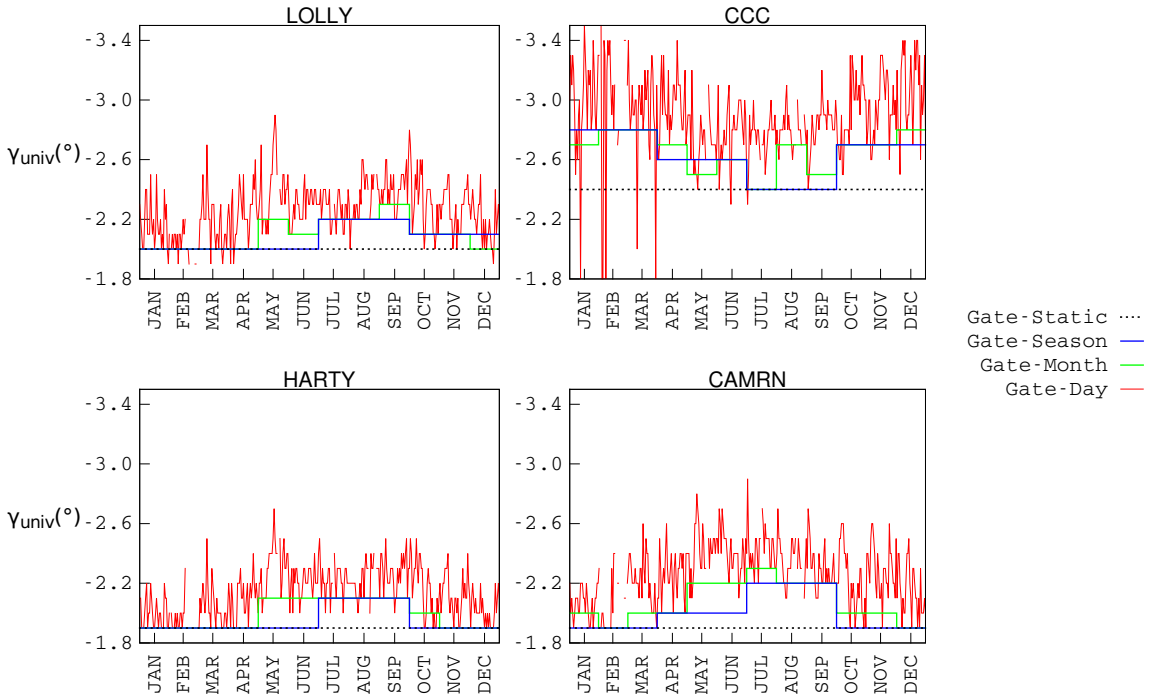

Figure 8. Values of γ_{univ} selected for the Gate-Static, Gate-Season, Gate-Month, and Gate-Day adaptations of Universal FPA.

V.E. Fuel Burn Comparison

Comparison of the three strategies in terms of their fuel burn merits is a necessary step in a benefit assessment. Other aspects of the comparison of the three strategies include the cost of implementation, which is beyond the scope of this paper. Another interesting comparison would be the fuel burn merit with any strategy against current-day operations. Since the strategies are expected to support EDA, their fuel burn benefit tends to be compounded with EDA's fuel benefit. An experimental design that would separate the benefit of the strategies from the benefit of EDA is left for future work.

To facilitate the fuel-burn comparison, results are presented in terms of the average fuel burn per flight, over the year's worth of JFK traffic data, relative to the minimum-fuel solution of Min-Fuel FPA. In this way, the results will show how close the simpler strategies, Universal FPA and Descent-Speed FPA, and their adaptations can come to the minimum-fuel solution without requiring real-time pilot-controller communication of FPA just prior to the top of descent.

The fuel burn comparison was based on trajectories spanning from the freeze horizon before the top-of-descent to the metering fix, and therefore has contributions from both the cruise and the descent segments. Figure 10 shows the extra fuel burn per flight computed for Universal FPA and Descent-Speed FPA. Overall, two interesting observations can be made. First, even the simplest strategy, a single static FPA adapted for JFK, has the potential to come within 21.5 lbs of the minimum-fuel solution for each flight on average. This 21.5 lbs represents the potential benefit of the Min-Fuel FPA solution. To put this into perspective, this represents approximately 4% of the fuel burn for a typical small-jet arrival transitioning over a 160 nmi segment from cruise to the TRACON boundary. This of course assumes that the modeled winds aloft and traffic conditions used for parameter selection are reasonably accurate.

To see the potential impact of directional and temporal adaptations on the fuel efficiency of Universal FPA and Descent-Speed FPA, consider the Universal FPA results on Figure 10. Adapting the universal "airport" FPA to season, month and day has the potential of reducing that extra 21.5 lbs of fuel per flight by 12%, 21%, and 38%, respectively. Relative to the Airport-Static adaptation, adaptation to the arrival gate only slightly reduces the "extra" 21.5 lbs of fuel per flight by 6%. In other words, publishing a universal FPA for each of the four gates will recover only 6% of the difference between the Aircraft-Specific adaptation of Universal FPA and the minimum fuel solution. Adaptation to gates becomes more effective when combined

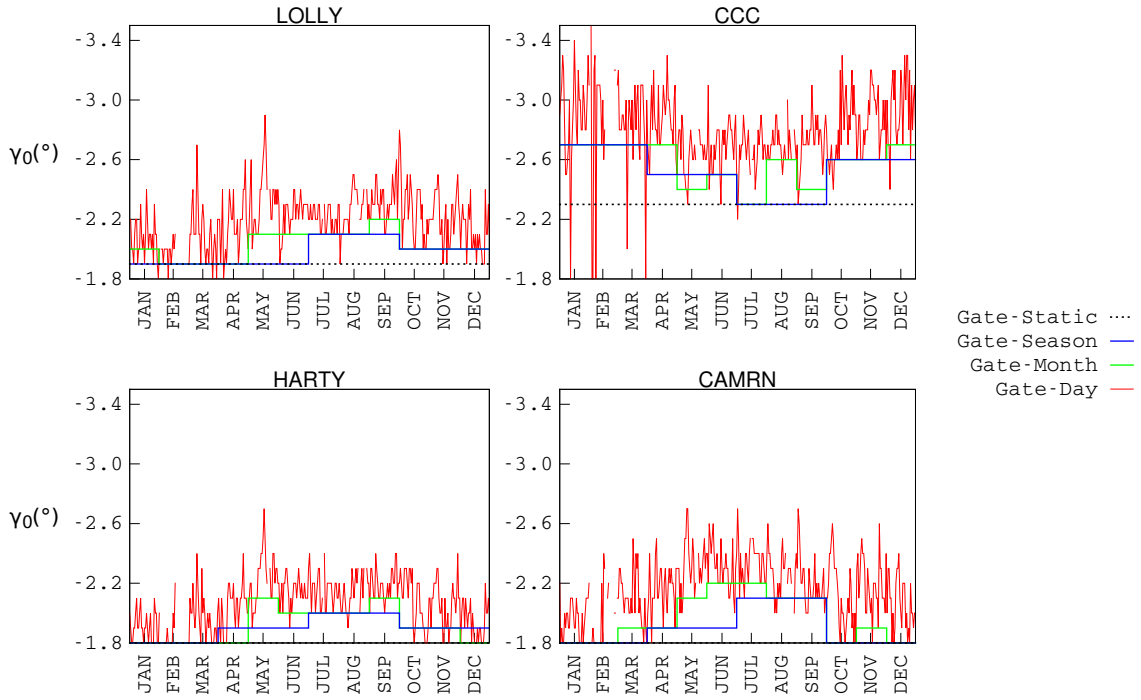

Figure 9. Values of γ_0 selected for the Gate-Static, Gate-Season, Gate-Month, and Gate-Day adaptations of Descent-Speed FPA.

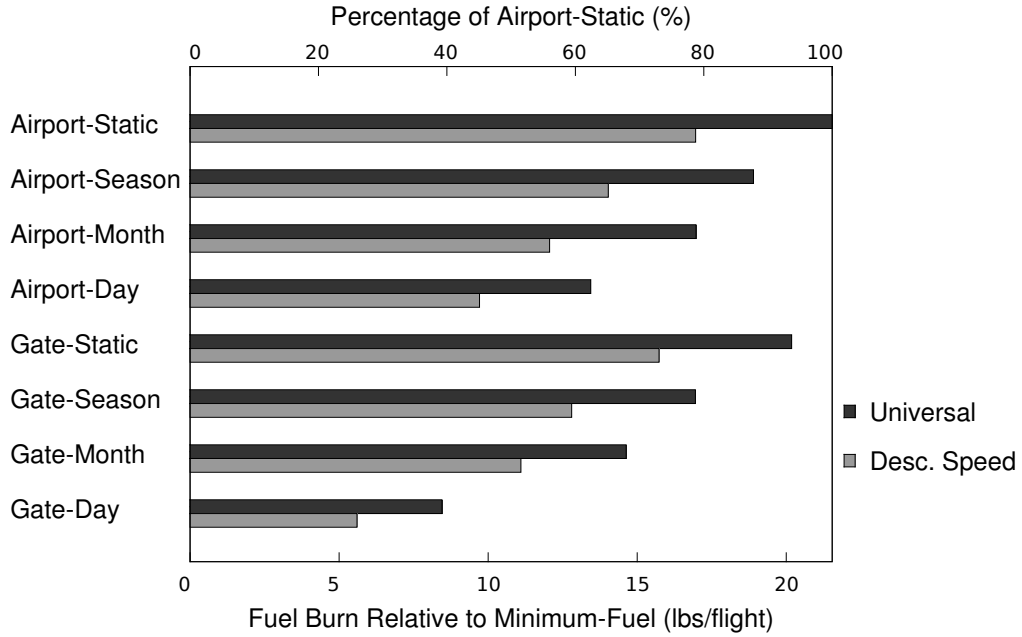

Figure 10. Extra fuel burn calculated for eight adaptations of Universal FPA and Descent-Speed FPA.

with finer granularity of timespan, as the Gate-Season, Gate-Month, and Gate-Day adaptations reduce the extra fuel burn from the corresponding airport-specific adaptations by 11%, 14%, and 38%, respectively. The combined adaptation of a universally fixed FPA for each arrival gate, for each day of operations, recovers about 61% of the fuel savings of the minimum-fuel solution for each flight.

By "adapting" to the descent speed, Descent-Speed FPA is essentially a surrogate adaptation for metering

delay, one of the primary factors being considered in this analysis. As such, this strategy was anticipated to yield a fair amount of benefit under metering conditions. The results indicate that Descent-Speed FPA contributes a 21% reduction in the 21.5 lbs of extra fuel burn over Universal FPA for the Airport-Static case. In considering the overall results for Descent-Speed FPA shown in Figure 10, both the directional and temporal adaptations yield similar improvements in fuel efficiency ranging from 22% to 29% among the types of adaptation. The combined effect of Descent-Speed FPA with both directional and temporal adaptation has the potential to achieve 74% of the Min-Fuel FPA benefit.

VI. Comparison of JFK and DFW Results

Comparison of the extra fuel burn between JFK and DFW sheds light on the major factors that affect the relative merits of the three strategies. The following discussion focuses on results for Universal FPA for JFK and DFW, with the results for DFW taken from previous work.[9] Descent-Speed FPA's fuel burn follows the same pattern and hence is not discussed here. Figure 11 compares the extra fuel burn of Universal FPA between JFK and DFW. The first observation is that the values of the extra fuel burn for the four

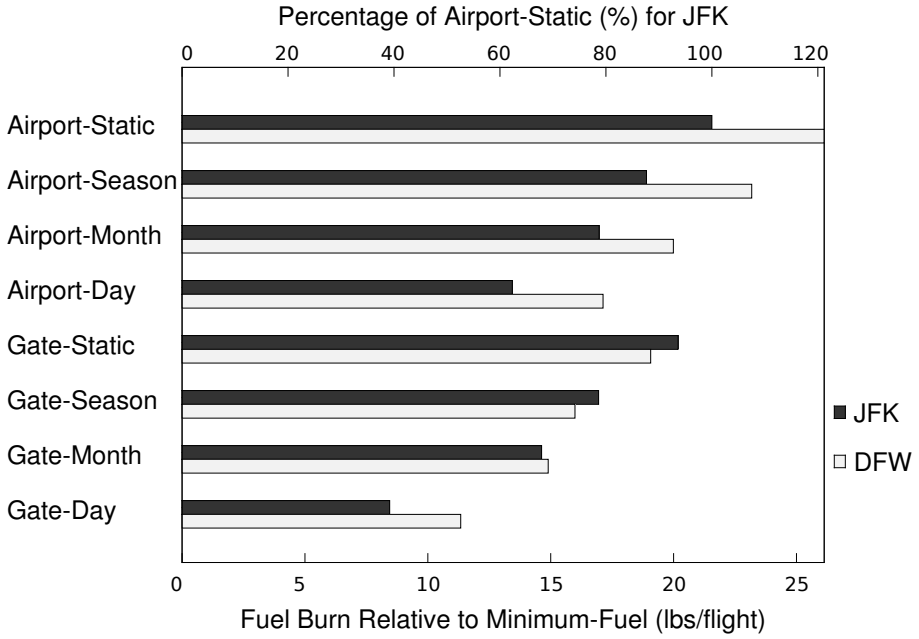

Figure 11. Comparison of Universal FPA's extra fuel burn between DFW and JFK.

airport-specific adaptation types for JFK are consistently less than those for DFW by 15% to 20%. A second observation is the relative ineffectiveness of the gate-specific adaptations for JFK, especially for the Gate-Static adaptation. While the gate-specific adaptations for DFW reduce the extra fuel burn from the corresponding airport-specific adaptations by 25% to 34%, the Gate-Static adaptation for JFK reduced only 6% of the Airport-Static extra fuel burn.

To determine each gate's contribution to the ineffectiveness of the Gate-Static adaptation for JFK, the extra fuel burn for each gate was examined and listed in Table 5. An average of the four values of extra fuel

Table 5. The extra fuel burn for each gate of JFK for the Gate-Static adaptation

	JFK		JFK+AL	
Gate	Extra Fuel Burn (lbs)	FPA (°)	Extra Fuel Burn (lbs)	FPA (°)
CCC	11.82	-2.4	11.82	-2.4
CAMRN	40.47	-1.9	40.47	-1.9
HARTY	7.97	-1.9	**38.63**	-1.9
LOLLY	8.55	-2.0	**31.45**	-2.0

burn, weighted by the number of flights (See Table 4), would yield the average extra fuel burn of 20.2 lbs in Figures 11 and 10. The extra fuel burn for CAMRN is above 40 lbs, more than three times higher than the extra fuel burn for any of the other three gates. This high extra fuel burn is definitely related to the very shallow FPA of -1.9° selected for CAMRN. However, HARTY also had -1.9° selected but resulted in an extra fuel burn of 8 lbs only.

The difference between the extra fuel burn of CAMRN and HARTY was due to the short descent segments required for capturing the high-altitude constraints for HARTY and LOLLY, which reduced the extra fuel burn significantly. To demonstrate the effects of the descent segment on the extra fuel burn, a modification to the JFK configuration/constraints, denoted as +AL, was used in another simulation that lowered the altitude constraint for HARTY and LOLLY from 21,000 ft and 20,000 ft, respectively, to 12,000 ft. The results are shown on the right side of Table 5. The modification increased the extra fuel burn for HARTY and LOLLY by more than three times, approaching that for CAMRN.

Another factor to consider is that the directions of the arrival flights to JFK are very different than those to DFW. While three quarters of the arrival flights to JFK are from the west, two-thirds of the arrival flights to DFW are from the east.[9] This means most arrival flights to JFK experience tailwinds, while most arrival flights to DFW experience headwinds. The selected FPA for a tailwind-dominant gate is usually shallower and farther from the minimum-fuel FPA of some individual flights, because it had to be shallow enough to be flyable for 99% of flights. The selected FPA for a headwind-dominant gate, on the contrary, is usually close to the minimum-fuel FPA of many flights. Therefore, the extra fuel burn for a tailwind-dominant gate is usually higher than that for a headwind-dominant gate. Since tailwinds dominate the gates CAMRN, HARTY, and LOLLY, the extra fuel burn for these three gates is much higher (in the +AL configuration) than the value for CCC, the only gate where headwinds dominate.

In addition to the +AL configuration, two more modifications of the configuration were used to further isolate the contributions of various factors contributing to the difference of extra fuel burn between JFK and DFW. All three modifications are listed in Table 6. The +CR aligns the average ground course of the

Table 6. Modifications to the JFK configuration used for calculating the extra fuel burn

Name	Comment
+AL	Reduced altitude constraints for LOLLY and HARTY
+CR	Aligned average ground course for each gate to that of DFW
+WD	Swapped the RUC wind out for that for DFW

arrival flights for a specific gate to JFK with a gate to DFW, by moving the aircraft's initial position while fixing its distance to the gate. With this modification, the flights to CCC, CAMRN, HARTY, and LOLLY are aligned in terms of their average ground courses with those to the NE, SE, SW, and NW gates of DFW, respectively. The +WD swaps out the RUC wind estimates for JFK for the RUC wind estimates for DFW. This configuration would reveal the effect of the wind field on the relative fuel-burn merits of the three strategies.

Figure 12 shows the differences of extra fuel burn between JFK and DFW, averaged over the eight adaptation types, for various modified JFK configurations. The average percentage difference uses each of the eight extra fuel burn values for DFW as the reference and is defined by Equation 6.

$$\Delta P = 100 \times \frac{1}{8} \sum_{k=1}^{8} \frac{\Delta f_{k,\mathrm{JFK}} - \Delta f_{k,\mathrm{DFW}}}{\Delta f_{k,\mathrm{DFW}}}, \tag{6}$$

where ΔP is the average percentage difference and Δf_k is the extra fuel burn for adaptation k. The vertical error bar represents variation of the percentages of differences in the eight adaptation types. The increase in extra fuel burn in the +AL configuration was contributed largely by HARTY and LOLLY, with one example shown for the Gate-Static adaptation in Table 5. Adding +CR on top of +AL reduces the average difference from 50% above DFW to 24% above DFW. A closer look at the Gate-Static extra fuel burn with +AL+CR revealed that the extra fuel burn for CAMRN reduced significantly from 40.6 lbs to 17.0 lbs. This is largely due to the change of the average ground course of the arrival flights from 58° to 290°, turning the wind along the route from predominantly tailwinds to predominantly headwinds. Adding +WD on top of +AL and +CR further reduces the average difference from 24% above DFW to 12% above DFW. This is in agreement with the fact that the winds for DFW are weaker than those for JFK.

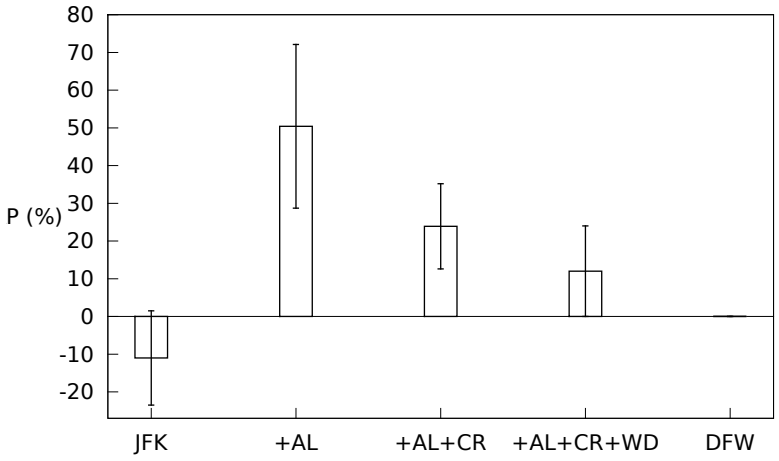

Figure 12. Universal FPA's average extra fuel burn difference relative to DFW using modified JFK configurations.

Other factors contribute to the difference of the extra fuel burn between JFK and DFW but are not further investigated. One noticeable factor is that the aircraft arriving at JFK are, on average, larger than those arriving at DFW. For example, the most frequent aircraft at JFK, E190, is larger than both the most frequent E135 and E145 observed for DFW. The resulting extra fuel burn per flight for JFK, therefore, will be larger than that for DFW with other factors being equal.

To summarize the discoveries in the section, three factors were investigated and found to contribute significantly to the relative fuel-burn merits of the three strategies:

- High-altitude constraints at JFK diminish the difference of fuel-burn merits between the three selection strategies.
- Arrival directions at JFK, predominantly from west, increase the difference of fuel-burn merits between the three selection strategies.
- Stronger winds at JFK increase the difference of fuel-burn merits between the three selection strategies.

VII. Conclusion and Future Work

This paper applied three strategies for choosing/defining the descent flight-path angles (FPAs) for small jets in transition airspace under metering conditions to the John F. Kennedy Airport (JFK). The three FPA selection strategies are:

1. Universal FPA - defines a universal FPA for all small jets arriving to an airport, gate, or route.
2. Descent-Speed FPA - defines different FPAs for different descent speeds.
3. Min-Fuel FPA - computes a minimum-fuel FPA for each flight, but requires communication of the FPA to the pilot in real time.

The three strategies vary in operational complexity. The Min-Fuel FPA strategy served as a reference point for the fuel-burn merits. One year's worth of traffic data arriving at JFK during 2011 was used for the analysis of the three strategies. The FPA of Universal FPA and the FPA function of Descent-Speed FPA were selected based on fuel burn and planned speed-brake usage of the meet-time trajectories computed for the flights.

Results showed that the Universal FPA strategy with its FPA adapted to the JFK Airport had 21.5 lbs of extra fuel burn relative to the Min-Fuel FPA solution for each flight on average. Adaptation of the FPA to the arrival-gate reduced the extra fuel burn per flight by 6%. Adaptation of the FPA to each day reduced the extra fuel burn per flight by up to 38%. Combining the directional and temporal adaptations reduced the extra fuel burn by 61%. The Descent-Speed FPA stratey, considered as a surrogate adaptation to the descent

speed, reduced the extra fuel burn per flight by 21%. The combined effect of the directional, temporal, and speed adaptation recovered 74% of extra fuel burn relative to the Min-Fuel FPA solution.

Three factors were investigated and found to contribute significantly to the difference of relative fuel-burn merits between the three strategies between JFK and DFW: The high-altitude constraints at JFK, directions of arrival, and winds. While the high-altitude constraints diminish the difference of the fuel-burn merits of the three strategies, the specific directions of arrival and winds of JFK augment the difference. The effects of these airport-specific conditions on the relative fuel-burn merits show the complexity of analyzing the economics of an FPA selection, and should assist in the design of a generic FPA selection procedure for a variety of airports.

The planned future work includes generalization of the FPA selection process to a third disparate airport that has weaker wind variations; possibly the Los Angeles International Airport (LAX). Another relevant analysis orthogonal to the airport adaptation is to define a "normalized" fuel-burn metric that removes the effects of high-altitude restrictions and aircraft size on the fuel-burn merits. It would be interesting to see if such a metric yields more universal results than the absolute fuel-burn difference.

References

[1]Coppenbarger, R. A., Mead, R. W., and Sweet, D. N., "Field Evaluation of the Tailored Arrivals Concept for Datalink-Enabled Continuous Descent Approach," *Journal of Aircraft*, Vol. 46, No. 4, July-August 2009, pp. 1200–1209.

[2]Novak, D., Bucak, T., and Radišić, T., "Development, Design and Flight Test Evaluation of Continuous Descent Approach Procedure in FIR Zagreb," *PROMET - Traffic & Transportation*, Vol. 21, No. 5, Sept. 2009, pp. 319–329.

[3]Clarke, J.-P. B., Ho, N. T., Ren, L., Brown, J. A., Elmer, K. R., Tong, K.-O., and Wat, J. K., "Continuous Descent Approach: Design and Flight Test for Louisville International Airport," *Journal of Aircraft*, Vol. 41, No. 5, 2004, pp. 1054–1066.

[4]"FAA Aerospace Forecast Fiscal Years 2012-2032," *Federal Aviation Administration*, 2011.

[5]Lauderdale, T. A., Cone, A. C., and Bowe, A. R., "Relative Significance of Trajectory Prediction Errors on an Automated Separation Assurance Algorithm," *Proceedings of the 9th USA/Europe Air Traffic Management R&D Seminar*, June 2011.

[6]Stell, L., "Prediction of Top of Descent Location for Idle-thrust Descents," *Proceedings of the 9th USA/Europe Air Traffic Management R&D Seminar*, June 2011.

[7]Coppenbarger, R. A., Nagle, G., Sweet, D., and Hayashi, M., "The Efficient Descent Advisor: Technology Validation and Transition," *Proceedings of the AIAA Aircraft Technology, Integration, and Opterations Conference*, AIAA-2012-5611, Sept. 2012.

[8]Swenson, H. N., Hoang, T., Engelland, S., Vincent, D., Sanders, T., Sanford, B., and Heere, K., "Design and Operational Evaluation of the Traffic Management Advisor at the Fort Worth Air Route Traffic Control Center," *Proceedings of the 1st USA/Europe Air Traffic Management R&D Seminar*, June 1997.

[9]Wu, M. G. and Green, S. M., "Strategies for Choosing Descent Flight Path Angles for Small Jets," *Proceedings of the AIAA Guidance, Navigation, and Control Conference*, AIAA-2012-4817, Aug. 2012.

[10]Wu, M. G. and Green, S. M., "Analysis of Fixed Flight Path Angle Descents for the Efficient Descent Advisor," NASA/TM-2011-215992, Nov. 2011.

[11]Sopjes, R., De Jong, P., Borst, C., Van Paassen, M., and Mulder, M., "Continuous Descent Approaches with Variable Flight-Path Angles under Time Constraints," *Proceedings of the AIAA Guidance, Navigation, and Control Conference*, AIAA-2011-6219, Aug. 2011.

[12]Benjamin, S. G., Brown, J. M., Brundage, K. J., Schwartz, B., Smirnova, T., Smith, T. L., Morone, L. L., and Dimego, G., "The Operational RUC-2. Preprints," *Proceedings of the 16th Conference on Weather Analysis and Forecasting*, Amer. Meteor. Soc., 1998, pp. 249–252.

[13]Landry, S., Farley, T., Foster, J., Green, S., Hoang, T., and Wong, G. L., "Distributed Scheduling Architecture for Multi-Center Time-Based Metering," *Proceedings of the AIAA Aviation Technology, Integration, and Opterations Conference*, AIAA-2003-6758, Nov. 2003.

[14]Lee, A. G., Bouyssounouse, X., and Murphy, J. R., "The Trajectory Synthesizer Generalized Profile Interface," *Proceedings of the 10th AIAA Aviation Technology, Integration, and Operations Conference*, AIAA-2010-9138, Sept. 2010.

[15]Slattery, R. and Zhao, Y., "Trajectory Synthesis for Air Traffic Automation," *Journal of Guidance, Control and Dynamics*, Vol. 20, No. 2, March 1997, pp. 232–238.

[16]Erzberger, H., Davis, T. J., and Green, S. M., "Design of Center-TRACON Automation System," *Machine Intelligence in Air Traffic Management, Andre Benoit, ed., AGARD CP-538*, Oct. 1993, pp. 11–1–11–12.

[17]Nuic, A., Poinsot, C., Iagaru, M.-G., Gallo, E., Navarro, F. A., and Querejeta, C., "Advanced Aircraft Performance Modeling for ATM: Enhancements to the BADA Model," *Proceedings of the IEEE/AIAA 24th Digital Avionics Systems Conference*, Nov. 2005.

[18]Coppenbarger, R. A., Lanier, R., Sweet, D., and Dorsky, S., "Design and Development of the En Route Descent Advisor (EDA) for Conflict-Free Arrival Metering," *Proceedings of the AIAA Guidance, Navigation, and Control Conference*, AIAA-2004-4875, Aug. 2004.